



1 **Diverging hydrological drought traits over Europe with global warming**

2

3 Carmelo Cammalleri*, Gustavo Naumann, Lorenzo Mentaschi, Bernard Bisselink, Emiliano Gelati,
4 Ad De Roo and Luc Feyen

5

6 European Commission, Joint Research Centre (JRC), 21027 Ispra (VA), Italy.

7 * Correspondence: carmelo.cammalleri@ec.europa.eu; Tel.: +39-0332-78-9869.

8

9 **Abstract**

10 Climate change is anticipated to alter the demand and supply of water at the earth's surface. Since
11 many societal impacts from a lack of water happen under drought conditions, it is important to
12 understand how droughts may develop with climate change. This study shows how hydrological
13 droughts will change across Europe with increasing global warming levels (GWL of 1.5, 2 and 3 K
14 above preindustrial temperature). We employ a low-flow index derived from river discharge
15 simulations of a spatially-distributed physically-based hydrological and water use model, which was
16 forced with a large ensemble of regional climate model projections under a high emissions
17 (RCP8.5) and moderate mitigation (RCP4.5) pathway. Different traits of drought, including
18 severity, duration and frequency, were investigated. The projected changes in these traits identify
19 four main sub-regions in Europe that are characterized by somehow homogeneous and distinct
20 behaviours with a clear southwest/northeast contrast. The Mediterranean and Boreal sub-regions of
21 Europe show strong, but opposite, changes at all three GWLs, with the former area mostly
22 interested by stronger droughts (with larger differences at 3 K) while the latter sees a reduction in
23 droughts. In the Atlantic and Continental sub-regions the changes are less marked and characterized
24 by a larger uncertainty, especially at the 1.5 and 2 K GWLs. Combining the projections in drought
25 hazard with population and agricultural information shows that with 3 K global warming an
26 additional 11 million people and 4.5 million ha of agricultural land will be exposed to droughts



27 every year, on average. These are mostly located in the Mediterranean and Atlantic regions of
28 Europe.

29

30 **Keywords:** climate change, drought, low flow index, Paris agreement.



31 **1. Introduction**

32 As a natural phenomenon, drought occurs in all climates due to a temporary lack of
33 precipitation, which can propagate through the different compartments of the water cycle (Van
34 Loon and Van Lanen, 2012). Drought conditions can be exacerbated by high temperatures, causing
35 an increase in evapotranspiration demand and soil water content draining (e.g., Teuling et al., 2013).
36 Their impacts can be further intensified in areas with an overexploitation of available water
37 resources (Van Loon and Van Lanen, 2013). The strong dependency of drought conditions on the
38 key meteorological forcing suggests likely effects of climate change on future drought severity,
39 duration and frequency, mainly through an alteration of the water balance dynamics (Stagl et al.,
40 2014).

41 Depending on the degree of penetration of drought into the water cycle, drought is commonly
42 classified into meteorological (e.g., precipitation), agricultural (e.g., soil moisture) and hydrological
43 (e.g., river discharge) (Wilhite, 2000). Different effects of climate change are likely to be observed
44 depending on the corresponding analysed indicators (Feng, 2017). In spite of the strong connection
45 between the socioeconomic impacts of droughts and negative soil moisture and river discharge
46 anomalies, fewer studies (e.g., Samaniego et al., 2018; Forzieri et al., 2014) have focused on these
47 typologies of droughts compared to meteorological events (e.g., Heinrich and Gobiet, 2012; Spinoni
48 et al., 2018). This relates mainly to the relative simplicity and lower input data requirements of
49 calculating meteorological drought indicators (i.e., Standardised Precipitation Index, SPI) compared
50 to agricultural and hydrological drought indices. This is also highlighted by the larger emphasis
51 placed on meteorological drought hazard in operational monitoring systems (Barker et al., 2016).
52 Scientific and practical interest in hydrological drought is motivated by the direct and indirect
53 impacts on several socioeconomic sectors, such as energy production, inland water transportation,
54 irrigated agriculture, and public water supply. In particular, streamflow drought complements
55 meteorological and soil moisture droughts thanks to its more rapid response to precipitation
56 aberrations compared to groundwater (Tallaksen and van Lanen, 2004).



57 With the raising awareness of climate change, a number of local and regional studies have
58 assessed the potential impacts of climate change on hydrological drought in recent years (e.g., Cervi
59 et al., 2018; Hellwig and Stahl, 2018; Nerantzaki et al., 2019; Rudd et al., 2019; Van Tiel et al.,
60 2018). Despite the high detail and insight on local processes these studies provide, their limited
61 spatial coverage and the use of different drought indicators, models and scenarios complicates the
62 understanding of large-scale patterns of changes. In spite of the value of continental-scale analyses,
63 few studies have looked at how hydrological droughts could develop across Europe with climate
64 change. They are typically based on pan-European hydrological models forced by climate
65 projections (Feyen and Dankers, 2009; Forzieri et al., 2014; Lehner et al., 2006; Marx et al., 2018;
66 Roudier et al., 2016), with ever improved representation of processes in the hydrological models,
67 including the effects of water use, more detail in the climate projections (by the use of higher
68 resolution regional climate models), and better accounting for climate uncertainty through multi-
69 model ensembles.

70 Most of past studies portrayed how droughts conditions across Europe could look at future
71 points in time (mid- or end- of century) for alternative scenarios of greenhouse gas emissions.
72 However, following the UNFCCC (United Nations Framework Convention on Climate Change)
73 Paris Agreement (UNFCCC, 2015) and the goal of limiting the increase in global average
74 temperature to well below 2 K above the pre-industrial level, the paradigm in climate change
75 studies has shifted from analysing the effects at specific future time windows to evaluating the
76 effect at given global warming levels (GWLs). To date, there are only few studies that provide
77 insights on how hydrological droughts could change at different GWLs. Roudier et al. (2016) used
78 three hydrological models forced with high resolution regional climate projections to evaluate
79 changes in 10- and 100-year streamflow drought events, with a focus solely on the 2 K scenario.
80 Marx et al. (2018) used three different hydrological models forced by coarse-resolution global
81 climate projections that were downscaled accounting for altitude effects in temperature and
82 precipitation. They used a simple annual 90-th percentile of river discharge as index, which is



83 representative of the low flow spectrum. Both studies do not take into account water consumption,
84 which is a key to represent feedbacks between droughts and human activities (Van Loon et al.,
85 2016).

86 To further deepen the understanding on this issue, we evaluate changes in hydrological
87 droughts across Europe between present climate and climate corresponding to different GWLs. We
88 look specifically at 1.5, 2 and 3 K global warming, which represent different climate change
89 mitigation targets. We use streamflow deficit as an indicator of drought as it represents the
90 integrated deficiency in water budget over the upstream catchment. The indicator is derived from
91 daily streamflow simulations for the pan-European river network, which are obtained with a
92 continental spatially-distributed hydrological and water use model forced with an ensemble of 11
93 bias-corrected regional climate projections for RCP4.5 and RCP8.5. We performed extreme value
94 analysis on the streamflow deficits in order to evaluate changes in drought traits, such as duration,
95 severity and frequency. In addition, spatial maps of present and future population and agricultural
96 land were combined with the drought projections in order to identify changes in streamflow drought
97 exposure.

98 **2. Materials and Methods**

99 **2.1 Climate forcing**

100 In this study, we used projections from 11 combinations of global and regional climate models
101 under two Representative Concentration Pathways (RCP4.5 and RCP8.5) obtained from EURO-
102 CORDEX (Jacob et al., 2014). The climate projections were adjusted for bias with a quantile
103 mapping approach (Dosio et al., 2012) using the observational dataset EOBSv10 (Haylock et al.,
104 2008). The analysis focuses on 30-year time windows centred on the year when the global models
105 project an increase in global average temperature of 1.5, 2 and 3 K above preindustrial temperature.
106 For these periods, drought characteristics were contrasted against those derived for the baseline
107 reference period (1981-2010). Outputs from both RCPs are merged, under the assumption that
108 between-pathway differences are generally much smaller than the within-pathway variability



109 (Mentaschi et al., 2020). It should be noted that only one model reaches 3 K warming for RCP4.5,
110 hence the model ensemble is composed by a total of 22 members for the 1.5 and 2 K GWLs and
111 only 12 members for the 3 K GWL.

112 **2.2 Hydrological modelling**

113 Simulations of daily river discharge (Q) were produced at 5×5 km spatial resolution over
114 Europe by forcing the LISFLOOD model (De Roo, 2000) with the bias-corrected climate
115 projections. LISFLOOD is a spatially-distributed physically-based hydrological model that
116 simulates all the main hydrological processes occurring in the land-atmosphere system, including
117 evapotranspiration fluxes, infiltration, soil water redistribution in the vadose zone, groundwater
118 dynamics, and surface runoff (Burek et al., 2013). The surface runoff generated in each cell is
119 channelled to the nearest river network cell by means of a routing component based on a 4-point
120 implicit finite-difference solution of the kinematic wave (Chow et al., 1988).

121 Water abstractions in LISFLOOD consist of five components: (manufacturing) industrial,
122 energy, livestock, domestic and irrigation water demand. Irrigation is estimated dynamically within
123 the model based on the required amount for crop transpiration that cannot be supplied by soil
124 moisture above the wilting point. Water demand in the other four sectorial components is derived
125 from country-level data (EUROSTAT, AQUASTAT) with different modelling and downscaling
126 techniques for each component (see Vandecasteele et al., 2014; Mubareka et al., 2013). Future
127 water use is based on projections of population, land use, energy demand and economic output of
128 sectors according to the EU economic, budgetary, and demographic projections (EC, 2015). The
129 Land-Use based Integrated Sustainability Assessment (LUISA) Territorial Modelling Platform was
130 used for the spatial downscaling of the socioeconomic drivers of present and future water use
131 (Jacobs-Crisioni et al., 2017). The population and land use projections are limited to 2050 and were
132 assumed static thereafter. A more elaborate description of the different water use modules can be
133 found in Bisselink et al. (2018).



134 **2.3 Drought indicator**

135 The hydrological drought index used in this study is analogous to the low-flow indicator used
136 in the European Drought Observatory (EDO) (Cammalleri et al., 2017). The key quantity is the
137 water deficit computed from an unbroken sequence of discharge (Q) values below a defined low-
138 flow threshold. We used the 85-th percentile, Q_{85} , derived for the present climate as a threshold
139 both in the present and future scenarios.

140 According to the theory of runs (Yevjevich, 1967), a continuous period with river flow values
141 below the defined low-flow threshold is considered as a drought event, of which the severity is
142 quantified by the total deficit (D , represented by the area enclosed by the threshold and the
143 streamflow time series). Other key traits of drought are the duration, quantified by the number of
144 drought days (N), and the temporal frequency of the events, which can be expressed as return period
145 (T).

146 In order to avoid the inclusion in the analysis of minor events, two post-processing corrections
147 were applied after selection of the events below the threshold: 1) consecutive events with an inter-
148 event time smaller than 10 days were pooled together (Zelenhasić and Salvai, 1987), and 2) small
149 isolated events (of duration less than 5 days) were removed from the analysis (Jakubowski and
150 Radczuk, 2004). The first of these corrections allows accounting for the statistical inter-dependency
151 of events that are close in time, whereas the second reduces the effects of the uncertainty in the
152 defined threshold by removing the events with discharge values very close to the threshold only for
153 a short period of time.

154 Following this definition, a sequence of drought events for both the baseline period and the
155 three GWLs were derived. Given the huge variability of D values across the European domain due
156 to differences in hydrological regimes and size of river basins, the changes in drought severity are
157 expressed as relative differences (%) from the values in the baseline period (1981-2010). The



158 empirical cumulative frequency of the D events was fitted according to the Pareto Type II
159 distribution with zero threshold (also known as Lomax distribution), formally expressed as:

$$160 \quad F(D; \alpha, \lambda) = 1 - \left(1 + \frac{D}{\lambda}\right)^{-\alpha} \quad (1)$$

161 where α and λ are the strictly positive shape and scale parameters, respectively, derived from the
162 sample according to the maximum likelihood method. The fitted distributions allow computing the
163 return period (T , inverse of the probability that one event is topped in any one year) associated to a
164 specific D value, or to be used in reverse to estimate the D value associated to a specific return
165 period. More details on the validation of the drought indicator over Europe and its operational
166 implementation in EDO can be found in Cammalleri et al. (2017)

167 **2.4 Population and agricultural land exposed to streamflow drought**

168 Droughts affect a large variety of socioeconomic sectors, including agriculture, water supply,
169 energy production and inland water transportation (Meyer et al., 2013), as well as causing losses of
170 ecosystem and biodiversity (Crausbay and Ramirez, 2017). The quantification of drought risk is a
171 challenging task (Naumann et al., 2015), and beyond the scope of this work. Here we quantified
172 how global warming could change exposure to streamflow drought in Europe. Apart from
173 agriculture, most of the sectors affected by drought are located close to where there is human
174 presence. As a result, we focus the exposure analysis on population and agricultural land. For the
175 baseline we used the map of agricultural areas from the CORINE land Cover (EEA, 2016) and the
176 population density from the LUISA Territorial Modelling Platform (Batista e Silva et al., 2013). For
177 future time slices the land use and population projections of LUISA were used..

178 The spatial data of population and agricultural land were summed over NUTS 2 statistical
179 regions (or equivalent for EU-neighbour countries according to Eurostat,
180 <https://ec.europa.eu/eurostat/web/nuts/statistical-regions-outside-eu>), and changes in the population
181 and agricultural land exposed to drought per year were computed by combing those data with the



182 median (over the NUTS 2) changes in drought frequency of a 10-year baseline event. This approach
183 assumes that, on average over a longer time window (such as a 30-year time slice), one-tenth of the
184 people and agricultural land of a NUTS 2 region are expected to be exposed each year to a present
185 10-year or more intense drought, and that the expected annual exposure changes accordingly to the
186 changes in drought frequency. Changes over NUTS 2 regions were further aggregate to country
187 scale.

188 **3. Results**

189 ***3.1 Evaluation of the changes in main drought traits***

190 ***3.1.1 Drought severity***

191 Figure 1 shows the ensemble-median relative change in severity of a 10-year drought between
192 the baseline and the GWLs, with positive (negative) values indicating a higher (lower) drought
193 severity with warming compared to the reference. The projected changes are considered robust
194 when at least 2/3 of the ensemble members agree on the sign of change (no-agreement otherwise).

195 The spatial maps depicted in Figure 1 highlight a strong divergence in the projected changes of
196 drought severity with warming over Europe, with four macro-regions (delimited in Figure 1 lower-
197 right panel) displaying somewhat homogeneous behaviour. In the Mediterranean sub-region (i.e.,
198 Iberian Peninsula, Italy, Greece and the Balkans) generally more severe droughts are projected,
199 whereas in the Boreal sub-area (i.e., Scandinavia peninsula and Baltic countries) drought severity
200 will reduce almost everywhere. The projected changes are less marked in two transition regions,
201 but, in general, they point towards more severe droughts in the Atlantic (i.e., British Isles, France,
202 Belgium and the Netherlands) and less severe droughts over the Continental sub-area (Germany,
203 Poland and eastern European countries). Overall, these patterns of change become stronger and
204 more robust with increasing warming.

205 The same rough subdivision, which is in line with the IPCC AR5 European macro regions
206 (Kovats et al., 2014) derived from a principal component analysis of 20 environmental-relevant



207 variables performed by Metzger et al. (2005), has been already observed even in previous early
208 studies at continental-scale (i.e., Feyen and Dankers, 2009; Lehner et al., 2006), and for this reason
209 it will be adopted in all the subsequent analyses.

210 The strongest increase in drought severity is projected for Portugal, Spain and Greece, where
211 the fraction of rivers with an increase in deficit of more than 50% at 3 K is 99, 80 and 75%,
212 respectively. If climate stabilizes at 2 K, streamflow drought severity is lower than at 3 K, but still
213 at least 50% higher than in the baseline for halve of the rivers of Portugal and Spain, and 35% of
214 Greece. Capping global warming at 1.5 K would further limit the increase in severity, with only 21,
215 20 and 14% of the rivers of Portugal, Spain and Greece experiencing an increase in drought severity
216 of more than 50%.

217 Over the Atlantic region (apart from Iceland), streamflow droughts will in general also become
218 more severe with global warming. The south of France shows a pattern towards more severe flow
219 deficits with warming that is similar to that projected for most of the Mediterranean. For the other
220 parts of the Atlantic sub-region the changes are less pronounced. Keeping warming to 2 K or below
221 would limit the increase in severity for most of the region to below 25% compared to the baseline.
222 At 3 K warming, the increase in severity could reach up to 50%. In some parts of the Atlantic sub-
223 region, such as the Seine river catchment in France, at lower levels of warming the climate models
224 do not agree on the sign of the change, or show a small trend towards less severe droughts. Yet,
225 with stronger warming the signal of change reverses towards more severe droughts.

226 Over most of the Continental sub-region there is a trend towards less severe droughts with
227 global warming. On the one hand, this trend is somewhat more pronounced in upstream Danube
228 tributaries that drain the Alps to the east. In many downstream Danube tributaries in Hungary,
229 Romania and Bulgaria, on the other hand, streamflow droughts are projected to become more severe
230 (in agreement with the results reported in Stagl and Hattermann, 2015). At low levels of global
231 warming (1.5 and 2 K) most of Germany will experience less severe droughts. At high levels of



232 warming (3 K), however, western parts of Germany will experience and inverse trend while the rest
233 shows a large uncertainty in the projected changes. In contrast to most of the Continental sub-area,
234 streamflow drought severity will increase with global warming over Denmark.

235 Finally, in most of the Boreal region, streamflow drought deficits will become progressively
236 less severe with warming. At 3 K warming streamflow droughts could be half as severe compared
237 to the baseline, with few notable exceptions in southern Sweden.

238 **3.1.2 Drought duration**

239 Figure 2 shows the fraction of each sub-region (presented in the lower-right panel of Figure 1)
240 for which a certain degree of change in drought duration is projected for the different warming
241 levels. There is a clear upward warming-induced trend in the fraction of the Mediterranean sub-
242 region that will be exposed to longer droughts. When keeping global warming limited to 1.5 K,
243 droughts are projected to last more than 10-days longer per year in about 45% of the Mediterranean,
244 with a prolongation above one month/year in less than 5% of the area. At 3 K warming, however,
245 streamflow droughts will last at least 10 days/year longer in 70% of the area and nearly half of the
246 sub-region could face an increase in drought duration of at least 30 days/year.

247 An upward, but less pronounced, trend in drought duration with global warming is also
248 projected for most of the Atlantic sub-region. At 1.5 K GWL, the area with a decrease (about 38%)
249 in drought duration is slightly larger than the area with an increase (about 26%), with no clear signal
250 in about one third of the domain. With higher levels of warming, the area with a shorter drought
251 duration shrinks, while the fraction of land that will face longer droughts steadily expands. At 3 K
252 GWL, droughts will last longer in about 80% of the sub-region, hence similar to what can be
253 observed for the Mediterranean. Yet, for only 13% of the area, drought duration is expected to
254 increase by more than a month/year.

255 In the Continental sub-region, the area that shows a decrease in drought duration is around 80%
256 at 1.5 K, which slightly reduces in extent with increasing warming. Yet, over this area droughts will



257 progressively shorten with further warming. At 3 K warming, droughts will last at least 10, 20 and
258 30 days shorter over more than 60, 40 and 20% of the region, respectively. Drought duration is
259 projected to increase over a small part (10% at 3 K) of the domain, mainly corresponding to
260 Bulgaria.

261 Over the Boreal sub-region, droughts are projected to become shorter with global warming over
262 practically the whole domain. At 1.5 K warming, droughts will last at least one month/year shorter
263 in 25% of the area, which grows to 80% of the area at 3 K warming. For all sub-regions, the
264 fraction of area with no-agreement in future drought duration decreases with increasing global
265 warming, and this signal is very consistent among all the climate projections. At 3 K warming, less
266 than 10% of the domain under study will have no agreement in the direction of change in drought
267 duration.

268 **3.1.3 Drought frequency**

269 Figure 3 shows the frequency distribution of drought return periods for the three GWLs
270 corresponding to an event with a return period (T) of 10 years under baseline climate. In these plots,
271 values greater than 10 can be interpreted as a reduction in drought frequency (an event with $T = 10$
272 years in the baseline will become rarer), whereas values lower than 10 represent an increase in
273 drought frequency (an event with $T = 10$ years in the baseline will become more common).

274 The frequency distributions of T values for the Mediterranean (upper-left panel) show a clear
275 shift towards more recurrent droughts. At 1.5 K warming the peak value is around 8 years, which
276 further reduces to 7 and 6 years at 2 and 3 K warming, respectively. At 3 K warming the lower tail
277 of the distribution falls below 4 years. In nearly 10% of the rivers, drought deficits that in baseline
278 climate happen once in 10 years are expected to occur at least 2.5 times more frequent with 3 K
279 warming. In the Atlantic sub-region the central value also reduces with warming, yet the average
280 reduction is less pronounced than in the Mediterranean sub-area, with a median value around 7
281 years at 3 K warming. In the Continental region, droughts will in general become less frequent with



282 a central value of around 12 years at all warming levels, even if the fraction of river cells with an
283 increase in frequency (around 25% at 3 K) is larger than that with an increase in drought duration
284 (around 10% at 3 K, see Figure 2). In the Boreal sub-area the shift towards less frequent droughts is
285 much more pronounced, with future return periods concentrated around 20, 30 and 40 years for 1.5,
286 2 and 3 K warming, respectively.

287 In addition to the shifts in central value of the frequency distributions, it is possible to observe
288 an increase with warming in the spread around the central value for all regions. Additionally,
289 changes opposite to the general trend can be observed in all regions. For example, over very few
290 locations in the Mediterranean sub-region, such as some Alpine mountain drainage basins in
291 northern Italy, drought conditions could become less severe and frequent (see also drought severity
292 changes in Figure 1). In the Atlantic region, the small secondary peak of T values > 20 years
293 corresponds to areas where droughts are projected to occur less frequently with global warming,
294 such as Iceland and few tributaries from the Rhône that originate in the Alps (similarly to what was
295 observed on drought severity in Figure 1). Even in the Boreal region a small fraction of the sub-
296 domain shows an increase in drought frequency, while drought duration is projected to reduce
297 practically everywhere.

298 ***3.2 Population and agricultural land exposed to drought***

299 Figure 4 shows the changes with respect to the baseline in population exposed to streamflow
300 drought at country scale (percentage relative changes are also reported as numbers next to the bars).
301 Total changes for the four macro-regions and the entire domain (TOT) are summarised in Table 1.
302 Aggregated over the whole domain, about 1.5 million fewer people will be annually exposed to
303 drought at 1.5 K GWL compared to the baseline period, which reverses to an increase of about 2.5
304 and 11 million people/year compared to baseline human exposure at 2 and 3 K GWLs, respectively.
305 This is because at 1.5 K the increase in population exposed annually in the Mediterranean (2.4
306 million) and Atlantic (less than 0.1 million) sub-regions is outweighed by the reduction in exposure



307 in the Boreal (-0.6 million) and, most importantly, Continental (-3.4 million) sub-regions. In the
308 Mediterranean and Atlantic sub-regions there will be a progressive increase in population exposed
309 (up to a total of 15.8 million people/year for 3 K GWL over the two regions), while in the Boreal
310 and Continental combined human exposure to droughts remains roughly the same for all three
311 GWLs (i.e., -3.9, -5.4 and -4.7 million/year at 1.5, 2 and 3 K, respectively).

312 Spain is projected to have the largest absolute increase in population exposed to drought with
313 global warming, with an almost doubling (+3.8 million/year) of the number of people exposed to
314 drought each year at 3 K GWL. In relative terms, the relative increase in population exposure at 3K
315 is also high in Portugal (+81%), United Kingdom (+58%) and France (+52%). The largest absolute
316 decrease in population exposed is observed for Germany at 1.5 and 2 K GWL (-1.8 and -1.7 million
317 people/year) and Poland at 3 K GWL. The transition of several areas in Germany from a decrease in
318 drought to uncertain conditions (see as an example western Germany in Fig. 1) explains the lower
319 number of exposed people at 3 K (-0.9 million people/year) compared to Poland (-1.2 million
320 people/year). The strongest reduction in population exposure in relative terms is observed for
321 Norway, Iceland and Lithuania (up to 65, 87 and 85%, respectively).

322 Exposure of agricultural land (Figure 5 and Table 2) shows similar trends as for population.
323 Aggregated over Europe, the change in exposure is balanced in the exposed agricultural land at 1.5
324 K GWL (net increase of 0.1 million ha/year), whereas at higher warming levels exposure of
325 agricultural land increases to 1.2 and 4.5 million ha/year at 2 and 3 K, respectively. This can be
326 explained by the steady increase in agricultural land exposed to drought in the Mediterranean and
327 Atlantic sub-regions (up to 6 million ha/year combined at 3 K), which is not counterbalanced at the
328 highest warming by the agricultural land being less exposed to drought in the Boreal and the
329 Continental sub-regions (-1.3 million ha/year at 1.5 K and -1.5 million ha/year at 3 K). In absolute
330 numbers, Spain shows the largest increase in the agricultural land exposed at all GWLs, with an
331 additional 0.9 million ha/year at 1.5 K to 2.6 million ha/year at 3 K (corresponding to a relative
332 increase of about 35 and 97%, respectively). Relative changes are also quite notable for other



333 Mediterranean countries, such as Portugal and Greece, reaching almost 120 and 77% at 3 K,
334 respectively.

335 **4. Discussion**

336 The projections of severity, duration and frequency underline some common features in future
337 streamflow drought in Europe. The uncertainty in the projections is more marked at the 1.5 and 2 K
338 GWLs, whereas patterns are more statistically robust at higher warming, as also observed by Marx
339 et al. (2018) for minimum flows. The magnitude of the observed changes increases in general with
340 warming for all the drought traits, with only limited areas interested by an inversion in the trend.
341 The main pattern is a strengthening of the dichotomy between southern but also western parts of
342 Europe that will become more prone to droughts and a wetting north. This is in line with other
343 studies that projected streamflow droughts focusing on specific temporal horizons (Lehner et al.,
344 2006; Feyen and Dankers, 2009; Stahl et al., 2012; Forzieri et al., 2014) or on agricultural (e.g.,
345 Samaniego et al., 2018) and meteorological (e.g., Gudmundsson and Seneviratne, 2016; Spinoni et
346 al., 2018) droughts. Hence, there is growing consensus in the community on the main patterns of
347 climate-induced changes on drought conditions in Europe.

348 Overall, the Mediterranean sub-region shows the strongest negative change, with droughts
349 projected to become more severe, last longer and happen more frequently already at 1.5 K GWL.
350 The combined effects of increasing temperature and decreasing summer precipitation (Vautard et
351 al., 2014) will result in a further exacerbation of water deficits in an area already prone to limited
352 water resources. This is in agreement with global studies that identify the Mediterranean as a hot
353 spot for climate change, even if the targets set by the Paris agreement will be met (Gu et al., 2020),
354 as well as with the potential occurrence of mega droughts in major Iberian water resource regions
355 (Guerreiro et al., 2017).

356 Symmetrically, the Boreal sub-region will experience a general reduction in drought, as the
357 increase in precipitation will outweigh the increase in evaporative demand due to elevated



358 temperatures (Jacob et al., 2018). Over this region, similarly to the Alps (Donnelly et al., 2017),
359 increasing winter precipitation and higher temperatures results in higher winter flows, when river
360 flows are typically at their lowest (Gobiet et al., 2014).

361 In the other two sub-regions the projections are less uniform, with more variation in the signal
362 and robustness of the projections with global warming. In the Atlantic sub-region the increase in
363 droughts at 3 K is less pronounced compared to the Mediterranean, but similarly robust, while at
364 lower warming levels there is large uncertainty in the projections. In some river basins, such as the
365 Seine in France, a positive (i.e., less droughts) or uncertain trend is projected for low levels of
366 global warming, while at higher levels of warming drought conditions are projected to worsen. This
367 is related to the fact that at higher levels of warming the atmospheric demand (evapotranspiration)
368 rises faster than supply due to the combination of a strong rise in temperature and a slight or
369 uncertain increase in annual precipitation and a decline in summer precipitation (Kotlarski et al.,
370 2014).

371 In the Continental sub-region the overall decrease in droughts is rather inhomogeneous in
372 strength. In upstream Danube tributaries draining the Alps there is a strong trend towards less
373 severe droughts as winter flows increase due to changes in snow accumulation and melt caused by
374 increased winter precipitation and higher temperatures (Forzieri et al., 2014; Marx et al., 2018). In
375 downstream reaches of the Danube, more severe droughts are projected due to a reduction in
376 summer flows caused by an increased evaporative demand and less precipitation. Also in Germany,
377 the trend towards less severe droughts for the Paris warming targets is reversed at higher warming
378 as the increasing natural and human demand in drier summers outbalance higher annual supply.
379 This is the case especially in western parts of Germany such as downstream reaches of the Rhine
380 (Bosshard and Kotlarski, 2014).

381 This shows that the projected trends relate to the interplay between supply (precipitation),
382 atmospheric demand (evapotranspiration) and human water use. Dosio and Fischer (2018) showed



383 that precipitation will increase over most continental and northern parts of Europe (by +10-25% at 3
384 K), but to a lesser extent in summer months (changes with 3 K between -5% at middle latitudes of
385 Continental Europe to +10-15% at higher latitudes in the Boreal region), when natural and human
386 demand are highest. In some catchments, short duration droughts could happen more frequently
387 when summer supply does not change drastically but natural demand grows due to rising
388 temperatures in combination with high human demand. In the mostly high-regulated basins in
389 Europe, accounting for water uses and its temporal evolution is key in studying streamflow drought
390 in the anthropocene, when both natural and human induced factors influence drought propagation
391 even further (Van Loon et al., 2016). Longer drought events reflect imbalances in precipitation over
392 longer time spans in which possible imbalances between supply and demand over summer are
393 counter balanced by increased subsurface storages at the start of the summer season due to elevated
394 precipitation amounts in the other seasons.

395 **5. Summary and Conclusions**

396 This study analysed how the main characteristics of hydrological droughts will change over
397 Europe due to global warming. Projections in drought severity, duration and frequency based on
398 river water deficits highlight some common features and spatial patterns in future drought
399 conditions across Europe. The Mediterranean sub-region, which already suffers most from water
400 scarcity, will experience the strongest negative effects of climate change on drought conditions.
401 With increasing global warming, streamflow deficits in this region will happen more frequently,
402 become more severe and last longer. Symmetrically, the Boreal sub-area will face a consistent
403 decrease in drought severity, duration and frequency.

404 In the Atlantic and Continental sub-regions the projections are less uniform, although over most
405 of the Atlantic drought conditions are projected to worsen, while they generally will become less
406 intense over Continental Europe. Despite the use of a large ensemble of climate models, there is still
407 a substantial uncertainty in the projections in these regions, even if changes at 3 K are mostly well



408 defined. The uncertainty is bigger for the 1.5 and 2 K GWLs, which suggests that there is still large
409 disagreement among the models in possible changes in drought conditions in these areas when
410 warming could be stabilised at the targets set in the Paris climate agreement.

411 The general patterns observed in this study are in line with other studies focused on specific
412 temporal horizons rather than warming levels (Forzieri et al., 2014; Spinoni et al., 2018; Stahl et al.,
413 2012), as well as with the results of Marx et al. (2018) on the simple daily streamflow percentile. In
414 addition to that, this study provides a comprehensive analysis of different traits of streamflow
415 droughts (i.e., severity, duration and frequency), it accounts for of the effects of human activities
416 through the modelling of water demand, and it focuses on policy-relevant GWLs. The findings
417 provide information that can be used as a basis to evaluate the implications at European scale of
418 climate mitigation policies.

419 In this regard, it is clear that with higher warming the changes in drought traits are more
420 marked, even if the spatial patterns of the areas with increasing/decreasing drought conditions are
421 rather similar for the three GWLs here analysed. The exposure analysis with population density and
422 agricultural land highlights how at lower warming levels positive and negative changes in exposure
423 are balanced across Europe. However, with higher levels of global warming the increase in
424 population and agricultural exposure in southern and western parts of Europe will outweigh the
425 effects of less severe droughts in the less populated north and most of continental and eastern
426 Europe. At 3 K warming this could result in an additional 11 million people and 4.5 million ha
427 exposed each year to drought conditions that currently are expected to happen once every 10 years
428 or less. The projected changes in exposure to drought will pose considerable challenges for
429 agriculture and water provision in densely populated and economically pivotal areas, especially in
430 southern Europe.



431 **References**

- 432 Barker, L.J., Hannaford, J., Chiverton, A., Svensson, C., 2016. From meteorological to hydrological
433 drought using standardised indicators. *Hydrol. Earth Syst. Sci.* 20, 2483-2505.
434 doi:10.5194/hess-20-2483-2016.
- 435 Batista e Silva, F., Gallego, J., Lavalle, C., 2013. A high-resolution population grid map for Europe.
436 *J. Maps* 9(1), 16-28. doi: 10.1080/17445647.2013.764830.
- 437 Bisselink, B., Bernhard, J., Gelati, E., Adamovic, M., Guenther, S., Mentaschi, L., De Roo, A.,
438 2018. Impact of a changing climate, land use, and water usage on Europe's water resources.
439 JRC Technical Reports, EUR 29130 EN, Publications Office of the European Union,
440 Luxembourg, 86 pp. doi:10.2760/847068.
- 441 Bosshard, T., Kotlarski, S., 2014. Hydrological climate-impact projections for the Rhine river:
442 GCM-RCM uncertainty and separate temperature and precipitation effects. *Hydrometeor.*
443 15, 697-713. doi:10.1175/JHM-D-12-098.1.
- 444 Burek, P., van der Knijff, J.M., De Roo, A., 2013. LISFLOOD: Distributed Water Balance and
445 Flood Simulation Model. JRC Technical Reports, EUR 26162 EN, Publications Office of
446 the European Union, Luxembourg, 142 pp. doi:10.2788/24719.
- 447 Cammalleri, C., Vogt, J., Salamon, P., 2017. Development of an operational low-flow index for
448 hydrological drought monitoring over Europe. *Hydrol. Sci. J.* 62(3), 346-358.
449 doi:10.1080/02626667.2016.1240869.
- 450 Cervi, F., Petronici, F., Castellarin, A., Marcaccio, M., Bertolini, A., Borgatti, L., 2018. Climate-
451 change potential effects on the hydrological regime of freshwater springs in the Italian
452 northern Apennines. *Sci. Total Environ.* 622-623, 337-348.
453 doi:10.1016/j.scitotenv.2017.11.231.
- 454 Chow, V.T., Maidment, D., Mays, L.W., 1988. *Applied Hydrology*. New York, McGraw-Hill.



- 455 Crausbay, S.D., Ramirez, A.R., 2017. Defining ecological drought for the twenty-first century. *Bull.*
456 *Am. Meteorol. Soc.* 2543-2550. doi:10.1175/BAMS-D-16-0292.1.
- 457 De Roo, A., Wesseling, C., Van Deursen, W., 2000. Physically based river basin modelling within
458 a GIS: the LISFLOOD model. *Hydrol. Process.* 14, 1981-1992. doi:10.1002/1099-1085.
- 459 Donnelly, C., Greuell, W., Andersson, J., Gerten, D., Pisacane, G., Roudier, P., Ludwig, F., 2017.
460 Impacts of climate change on European hydrology at 1.5, 2 and 3 degrees mean global
461 warming above preindustrial level. *Climatic Change* 143, 13-26. doi:10.1007/s10584-017-
462 1971-7.
- 463 Dosio, A., Fischer, E.M., 2018. Will half a degree make a difference? Robust projections of indices
464 of mean and extreme climate in Europe under 1.5°C, 2°C, and 3°C global warming. *Geoph.*
465 *Res. Letters* 45(2), 935-944. doi:10.1002/2017GL076222.
- 466 Dosio, A., Paruolo, P., Rojas, R., 2012. Bias correction of the ENSEMBLES high resolution
467 climate change projections for use by impact models: Analysis of the climate change signal.
468 *J. Geoph. Res. Atm.* 117(17). doi:10.1029/2012JD017968.
- 469 EC, 2015. The 2015 Ageing Report - Economic and budgetary projections for the 28 EU Member
470 States (2013-2060). European Commission. doi:10.2765/877631.
- 471 EEA, 2016. Corine Land Cover (CLC), Version 18.5.1. Release Date: 19-09-2016. European
472 Environment Agency. <https://land.copernicus.eu/pan-european/corine-land-cover>.
- 473 Feng, S., 2017. Why do different drought indices show distinct future drought risk outcomes in the
474 U.S. Great Plains? *J. Climate* 30, 265-278. doi: 10.1175/JCLI-D-15-0590.1.
- 475 Feyen, L., Dankers, R., 2009. Impact of global warming on streamflow drought in Europe. *J.*
476 *Geophys. Res.* 114, D17116. doi:10.1029/2008JD011438.



- 477 Forzieri, G., Feyen, L., Rojas, R., Flörke, M., Wimmer, F., Bianchi, A., 2014. Ensemble projections
478 of future streamflow droughts in Europe. *Hydrol. Earth Syst. Sci.* 18(1), 85-108.
479 doi:10.5194/hess-18-85-2014.
- 480 Gobiet, A., Kotlarski, S., Beniston, M., Heinrich, G., Rajczak, J., Stoffel, M., 2014. 21st century
481 climate change in the European Alps - A review. *Sci. Tot. Environ.* 493, 1138-1151.
482 doi:10.1016/j.scitotenv.2013.07.050.
- 483 Gu, L., Chen, J., Yin, J., Sullivan, S.C., Wang, H.-M., Guo, S., Zhang, L., Kim, J.-S., 2020.
484 Projected increases in magnitude and socioeconomic exposure of global droughts in 1.5 and
485 2 °C warmer climates. *Hydrol. Earth Syst. Sci.* 24, 451-472. doi:10.5194/hess-24-451-2020.
- 486 Gudmundsson, L., Seneviratne, S.I., 2016. Anthropogenic climate change affects meteorological
487 drought risk in Europe. *Environ. Res. Lett.* 11, 044005. doi:10.1088/1748-
488 9326/11/4/044005.
- 489 Guerreiro, S.B., Birkinshaw, S., Kilsby, C., Fowler, H.J., Lewis, E., 2017. Dry getting drier – The
490 future of transnational river basins in Iberia. *J. Hydrol. Reg. Studies* 12, 238-252.
491 doi:10.1016/j.ejrh.2017.05.009.
- 492 Haylock, M.R., Hofstra, N., Klein Tank, A.M.G., Klok, E.J., Jones, P.D., New, M., 2008. A
493 European daily high-resolution gridded data set of surface temperature and precipitation for
494 1950–2006. *J. Geoph. Res.* 113, D20119. doi:10.1029/2008JD010201.
- 495 Heinrich, G., Gobiet, A., 2012. The future of dry and wet spells in Europe: a comprehensive study
496 based on the ENSEMBLES regional climate models. *Int. J. Climatol.* 32(13), 1951-1970.
497 doi:10.1002/joc.2421.
- 498 Hellwig, J., Stahl, K., 2018. An assessment of trends and potential future changes in groundwater-
499 baseflow drought based on catchment response times. *Hydrol. Earth Syst. Sci.* 22(12), 6209-
500 6224. doi:10.5194/hess-22-6209-2018.



- 501 Jacob, D., Petersen, J., Eggert, B., Alias, A., Christensen, O.B., Bouwer, L.M., Braun, A., Colette,
502 A., Déqué, M., Georgievski, G., Georgopoulou, E., Gobiet, A., Menut, L., Nikukin, G.,
503 Haensler, A., Hempelmann, N., Jones, C., Keuler, K., Kovats, S., Kröner, N., Kotlarski, S.,
504 Kriegsmann, A., Martin, E., Van Meijgaard, E., Moseley, C., Pfeifer, S., Preuschmann, S.,
505 Radermacher, C., Radtke, K., Rechid, D., Rounsevell, M., Samuelsson, P., Somot, S.,
506 Soussana, J.-F., Teichmann, C., Valentini, R., Vautard, R., Weber, B., Yiou, P., 2014. EURO-
507 CORDEX: New high-resolution climate change projections for European impact research.
508 Reg. Environ Change 14(2), 563-578. doi:10.1007/s10113-013-0499-2.
- 509 Jacob, D., Kotova, L., Teichmann, C., Sobolowski, S.P., Vautard, R., Donnelly, C., Koutroulis,
510 A.G., Grillakis, M.G., Tsanis, I.K., Damm, A., Sakalli, A., Van Vliet, M.T.H., 2018. Climate
511 Impacts in Europe Under +1.5°C Global Warming. Earth's Future 6, 264-285.
512 doi:10.1002/2017EF000710.
- 513 Jacobs-Crisioni, C., Diogo, V., Perpiña Castillo, C., Baranzelli, C., Batista e Silva, F., Rosina, K.,
514 Kavalov, B., Lavallo, C., 2017. The LUISA Territorial Reference Scenario 2017: A technical
515 description. JRC Technical Reports, EUR 28800 EN, Publications Office of the European
516 Union, Luxembourg, 46 pp. doi:10.2760/902121.
- 517 Jakubowski, W., Radczuk, L., 2004. Estimation of hydrological drought characteristics
518 NIZOWKA2003 – Software Manual. In: L.M. Tallaksen and H.A.J. van Lanen, eds.
519 Hydrological Drought – Processes and estimation methods for Streamflow and groundwater.
520 Amsterdam: Elsevier Sciences B.V. [CD-ROM].
- 521 Kotlarski, S., Keuler, K., Christensen, O. B., Colette, A., Déqué, M., Gobiet, A., Wulfmeyer, V.,
522 2014. Regional climate modeling on European scales: A joint standard evaluation of the
523 EURO - CORDEX RCM ensemble. Geosci. Model Develop. 7(4), 1297-1333.
524 doi:10.5194/gmd-7-1297-2014.



- 525 Kovats, R., Valentini, R., Bouwer, L., Georgopoulou, E., Jacob, D., Martin, E., Rounsevell, M.,
526 Soussana, J.-F., 2014. Europe, In: *ClimateChange 2014: Impacts, Adaptation, and*
527 *Vulnerability. Part B: Regional Aspects. Contribution of Working Group II to the Fifth*
528 *Assessment Report of the Intergovernmental Panel on Climate Change*, Eds: Barros, V.R.,
529 C.B. Field, D.J. Dokken, M.D. Mastrandrea, K.J. Mach, T.E. Bilir, M. Chatterjee, K.L. Ebi,
530 Y.O. Estrada, R.C. Genova, B. Girma, E.S. Kissel, A.N. Levy, S. MacCracken, P.R.
531 Mastrandrea, L.L. White, pp. 1267–1326.
- 532 Lehner, B., Döll, P., Alcamo, J., Henrichs, T., Kaspar, F., 2006. Estimating the impact of global
533 change on flood and drought risks in Europe: a continental integrated analysis. *Clim.*
534 *Change* 75, 273-299. doi:10.1007/s10584-006-6338-4.
- 535 Marx, A., Kumar, R., Thober, S., Rakovec, O., Wanders, N., Zink, M., Wood, E.F., Pan, M.,
536 Sheffield, J., Samaniego, L., 2018. Climate change alters low flows in Europe under global
537 warming of 1.5, 2, and 3 °C. *Hydrol. Earth Syst. Sci.* 22, 1017-1032. doi:10.5194/hess-22-
538 1017-2018.
- 539 Mentaschi, L., Alfieri, L., Dottori, F., Cammalleri, C., Bisselink, B., De Roo, A., Feyen, L., 2020.
540 Independence of future changes of river runoff in Europe from the pathway to global
541 warming. *Climate*, 8, 22. doi:10.3390/cli8020022.
- 542 Metzger, M.J., Bunce, R.G.H., Jongman, R.H.G., Múcher, C.A., Watkins, J.W., 2005. A climatic
543 stratification of the environment of Europe. *Glob. Ecol. Biogeogr.* 14, 549–563.
544 doi:10.1111/j.1466-822X.2005.00190.x.
- 545 Meyer, V., Becker, N., Markantonis, V., Schwarze, R., van der Bergh, J.C.J.M., Bouwer, L.M.,
546 Bubeck, P., Ciavola, P., Genovese, E., Green, C., Hallagatte, S., Kreibich, H., Lequex, Q.,
547 Logar, I., Papyrakis, E., Pfuerscheller, C., Poussin, J., Przyluski, V., Thielen, A.H.,
548 Viavattene, C., 2013. Assessing the costs of natural hazards – state of the art and knowledge
549 gaps. *Nat. Hazard Earth Syst. Sci.* 13(5), 1351-1373. doi:10.5194/nhess-13-1351-2013.



- 550 Mubareka, S., Maes, J., Lavalle, C., De Roo, A., 2013. Estimation of water requirements by
551 livestock in Europe. *Ecosyst. Serv.* 4, 139-145. doi:10.1016/j.ecoser.2013.03.001.
- 552 Naumann, G., Spinoni, J., Vogt, J.V., Barbosa, P., 2015. Assessment of drought damages and their
553 uncertainties in Europe. *Environ. Res. Letters* 10(12). doi:10.1088/1748-
554 9326/10/12/124013.
- 555 Nerantzaki, S. D., Efstathiou, D., Giannakis, G.V., Kritsotakis, M., Grillakis, M.G., Koutroulis, A.
556 G., Tsanis, I.K., Nikolaidis, N.P., 2019. Climate change impact on the hydrological budget
557 of a large Mediterranean island. *Hydrol. Sci. J.* 64(10), 1190-1203.
558 doi:10.1080/02626667.2019.1630741.
- 559 Roudier, P., Andersson, J.C.M., Donnelly, C., Feyen, L., Greuell, W., Ludwig, F., 2016. Projections
560 of future floods and hydrological droughts in Europe under a +2°C global warming.
561 *Climatic Change* 135(2), 341-355. doi:10.1007/s10584-015-1570-4.
- 562 Rudd, A.C., Kay, A.L., Bell, V.A., 2019. National-scale analysis of future river flow and soil
563 moisture droughts: Potential changes in drought characteristics. *Clim. Change* 156(3), 323-
564 340. doi:10.1007/s10584-019-02528-0.
- 565 Samaniego, L., Thober, S., Kumar, R., Wanders, N., Rakovec, O., Pan, M., Zink, M., Sheffield, J.,
566 Wood, E.F., Marx, A., 2018. Anthropogenic warming exacerbates European soil moisture
567 droughts. *Nat. Clim. Change* 8, 421-426. doi:10.1038/s41558-018-0138-5.
- 568 Spinoni, J., Vogt, J.V., Naumann, G., Barbosa, P., Dosio, A., 2018. Will drought events become
569 more frequent and severe in Europe? *Int. J. Climatol.* 38(4), 1718-1736.
570 doi:10.1002/joc.5291.
- 571 Stagl J., Mayr E., Koch H., Hattermann F.F., Huang S., 2014. Effects of climate change on the
572 hydrological cycle in Central and Eastern Europe. In: Rannow S. and Neubert M. (eds.)
573 *Managing Protected Areas in Central and Eastern Europe Under Climate Change. Advances*
574 *in Global Change Research* 58. Springer, Dordrecht.



- 575 Stagl J., Hattermann F.F., 2014. Impacts of climate change on the hydrological regime of the
576 Danube river and its tributaries using an ensemble of climate scenarios. *Water* 7(11), 6139-
577 6172, doi:10.3390/w7116139.
- 578 Stahl, K., Tallaksen, L. M., Hannaford, J., and van Lanen, H. A. J., 2012. Filling the white space on
579 maps of European runoff trends: estimates from a multi-model ensemble. *Hydrol. Earth*
580 *Syst. Sci.* 16, 2035-2047. doi:10.5194/hess-16-2035-2012.
- 581 Tallaksen, L.M., Van Lanen, H.A.J., 2004. Drought as natural hazard: Introduction. In: L.M.
582 Tallaksen and H.A.J. Van Lanen, (eds.) *Hydrological Drought - Processes and estimation*
583 *methods for streamflow and groundwater*. Amsterdam: Elsevier Sciences B.V., 3-17.
- 584 Teuling, A.J., Van Loon, A.F., Seneviratne, S.I., Lehner, I., Aubinet, M., Heinesch, B., Bernhofer,
585 C., Grünwald, T., Prasse, H., Spank, U., 2013. Evapotranspiration amplifies European
586 summer drought. *Geophys. Res. Letters* 40(10), 2071-2075. doi:10.1002/grl.50495.
- 587 UNFCCC, 2015. The Paris Agreement. United Nations Framework Convention on Climate Change.
588 Available at: [https://unfccc.int/process-and-meetings/the-paris-agreement/the-paris-](https://unfccc.int/process-and-meetings/the-paris-agreement/the-paris-agreement)
589 [agreement](https://unfccc.int/process-and-meetings/the-paris-agreement/the-paris-agreement).
- 590 Vandecasteele, I., Bianchi, A., Batista e Silva, F., Lavalle, C., Batelaan, O., 2014. Mapping current
591 and future European public water withdrawals and consumption. *Hydrol. Earth Syst. Sci.* 18,
592 407-416. doi:10.5194/hess-18-407-2014.
- 593 Van Loon, A.F., Van Lanen, H.A.J., 2012. A process-based typology of hydrological drought.
594 *Hydrol. Earth Syst. Sci.* 16, 1915-1946. doi:10.5194/hess-16-1915-2012.
- 595 Van Loon, A.F., Van Lanen, H.A.J., 2013. Making the distinction between water scarcity and
596 drought using an observation - modeling framework. *Water Resour. Res.* 49, 1483-1502,
597 doi:10.1002/wrcr.20147.



- 598 Van Loon, A., Gleeson, T., Clark, J., Van Dijk, A.I.J.M., Stahl, K., Hannaford, J., Di Baldassarre,
599 G., Teuling, A.J., Tallaksen, L.M., Uijlenhoet, R., Hannah, D.M., Sheffield, J., Svoboda, M.,
600 Verdeiren, B., Wagener, T., Rangecroft, S., Wanders, N., Van Lanen, H.A.J., 2016. Drought
601 in the Anthropocene. *Nat. Geosci.* 9, 89-91. doi:10.1038/ngeo2646.
- 602 Van Tiel, M., Teuling, A.J., Wanders, N., Vis, M.J.P., Stahl, K., Van Loon, A.F., 2018. The role of
603 glacier changes and threshold definition in the characterisation of future streamflow
604 droughts in glacierised catchments. *Hydrol. Earth Syst. Sci.* 22(1), 463-485.
605 doi:10.5194/hess-22-463-2018.
- 606 Vautard, R., Gobiet, A., Sobolowski, S., Kjellström, E., Stegehuis, A., Watkiss, P., Mendlik, T.,
607 Landgren, O., Nikulin, G., Teichmann, C., Jacob, D., 2014. The European climate under a
608 2 °C global warming. *Environ. Res. Lett.* 9, 034006. doi:10.1088/1748-9326/9/3/034006.
- 609 Wilhite, D.A., 2000. Drought as a natural hazard: concepts and definitions. In: Wilhite D.A., (eds.)
610 *Droughts: Global Assessment*. London: Routledge, 3-18.
- 611 Yevjevich, V., 1967. An objective approach to definitions and investigations of continental
612 hydrological droughts. Colorado State University, Fort Collins, Hydrology Paper 23.
- 613 Zelenhasić, E., Salvai, A., 1987. A method of streamflow drought analysis. *Water Resour. Res.*,
614 23(1), 156-168. doi:10.1029/WR023i001p00156.

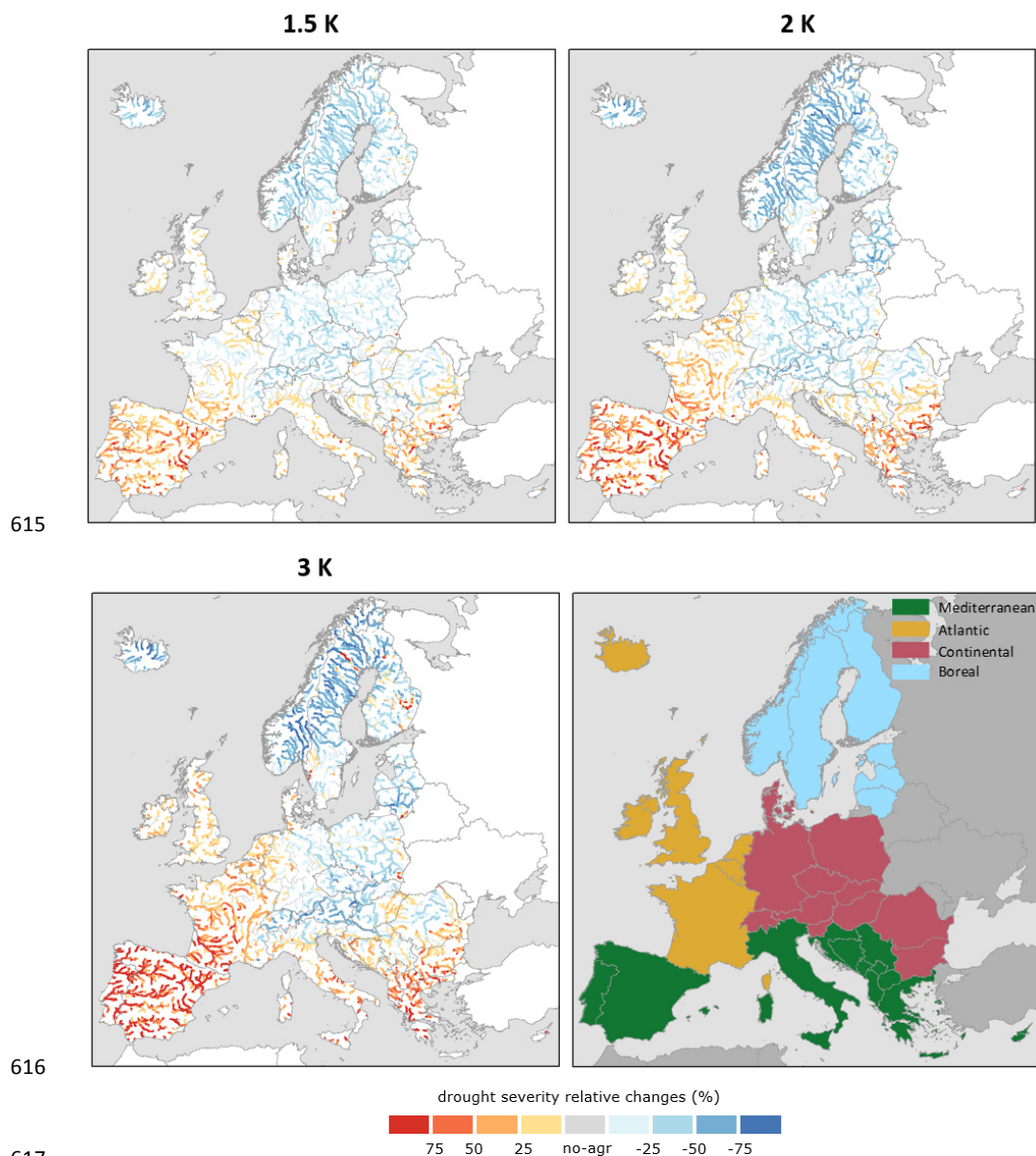
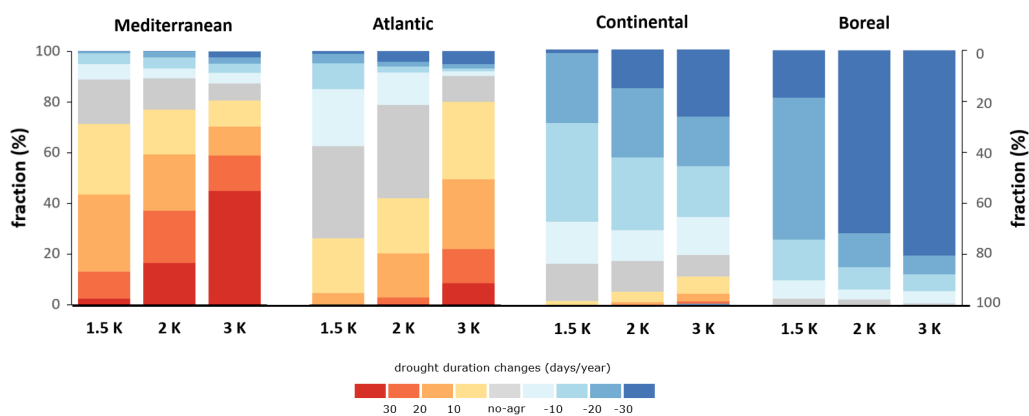
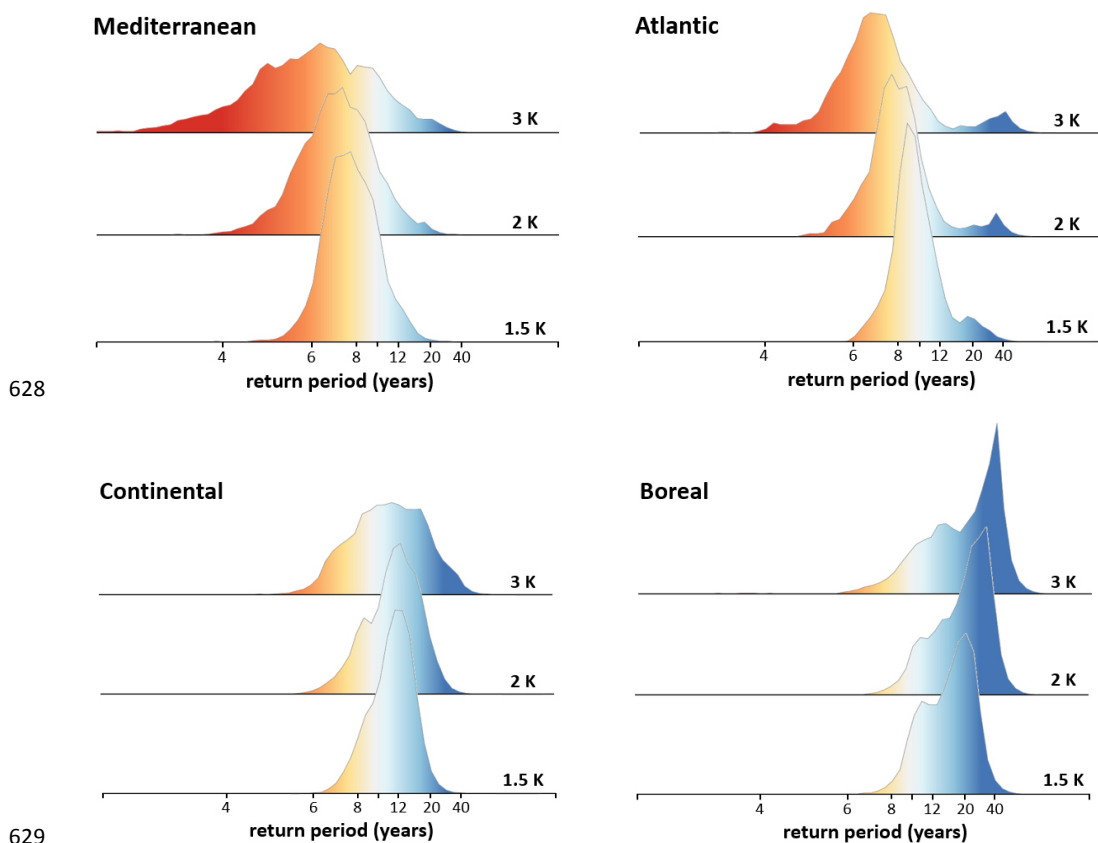


Fig. 1. Spatial distribution of the ensemble-median relative changes in drought severity (%) between reference period and the three GWLs (1.5 K in the upper-left panel, 2 K in the upper-right panel, 3 K in the lower-left panel). Positive values represent an increase in drought severity with warming. The no-agreement (no-agr) class identifies the cells where less than 2/3 of the climate ensemble members agree on the sign of the change. The lower-right panel represents the four sub-regions used for aggregation, which are in line with the IPCC AR5 European macro regions (Kovats et al., 2014).

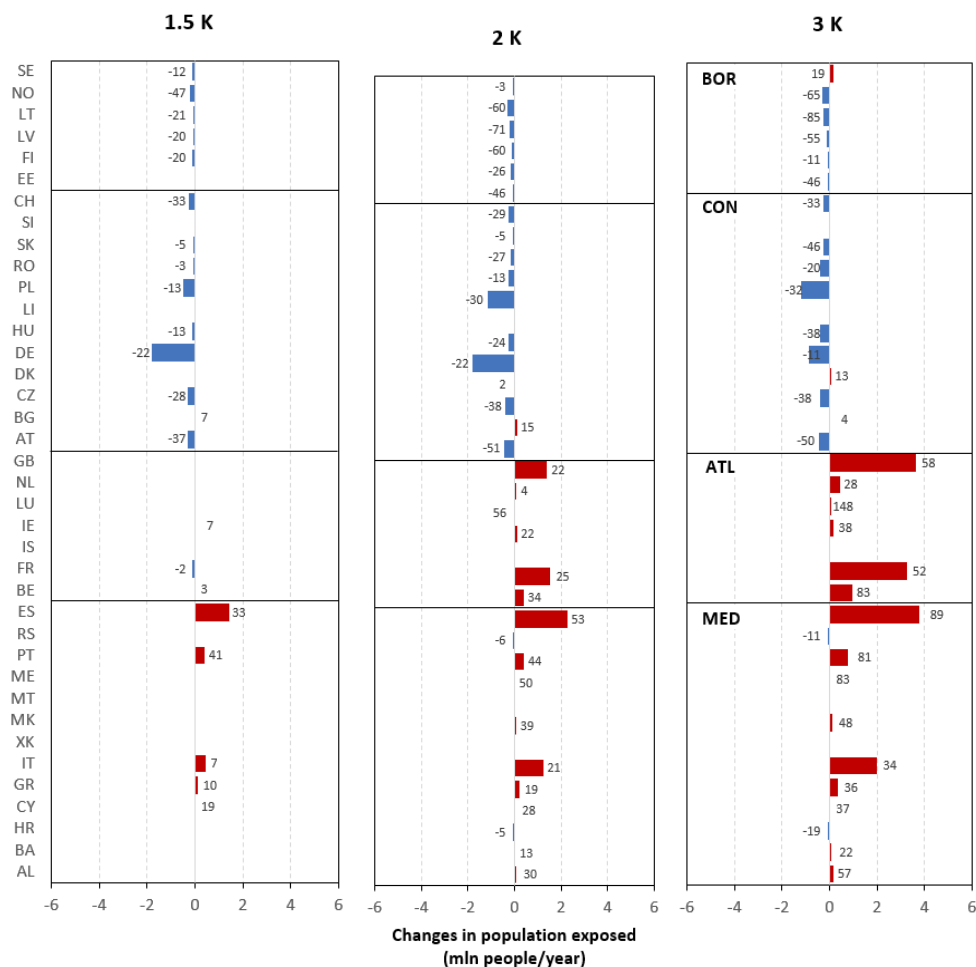


625

626 **Fig. 2.** Fraction of each sub-region within ranges of change in drought duration (days/year) for
627 different GWLs.

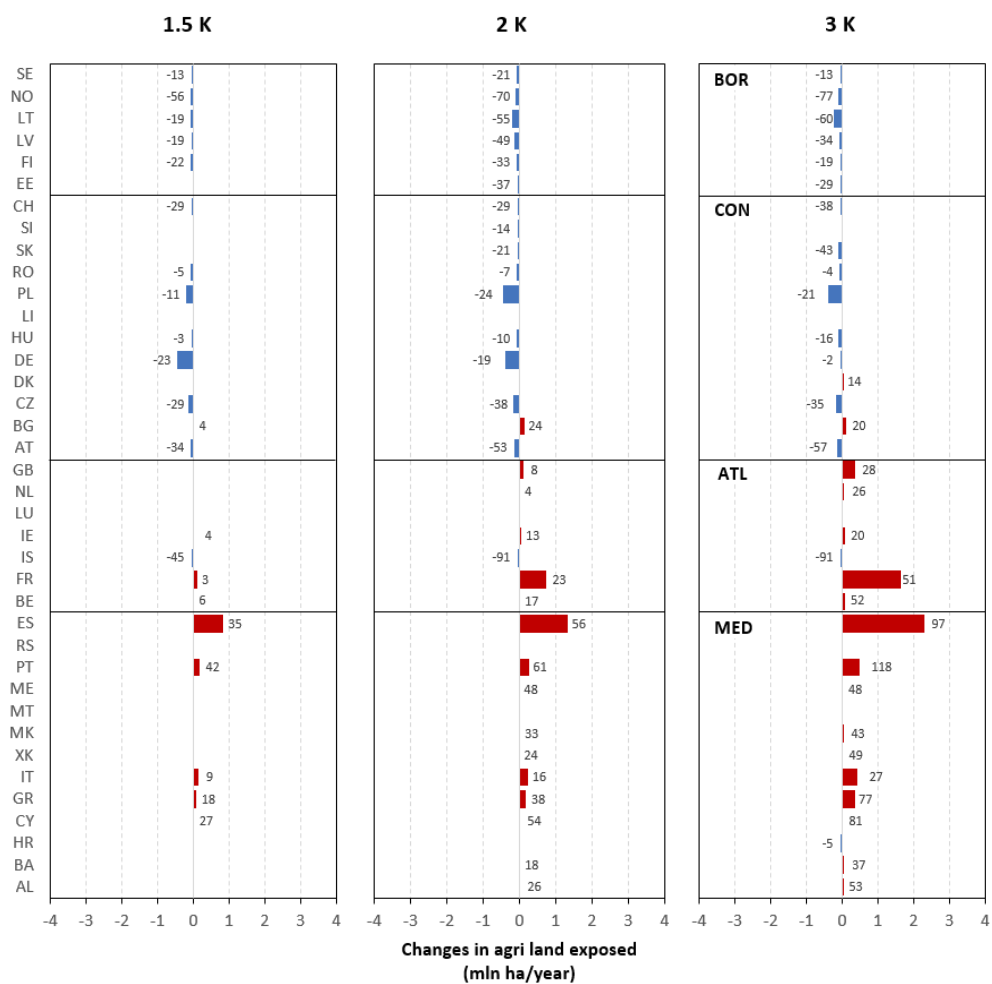


630 **Fig. 3.** Frequency distribution of the return period (years) for different GWLs corresponding to an
631 event with a return period of 10 years in the reference baseline. Values lower (higher) than 10
632 represent an increase (reduction) in drought frequency.



633

634 **Fig. 4.** Changes in population exposed per country (million people/year). Positive values indicate an
 635 increase in the population exposed. The numbers near the bars represent the percentage changes
 636 relative to the baseline (only if greater than 1%).



637

638 **Fig. 5.** Changes in agricultural land exposed per country (million ha/year). Positive values indicate
 639 an increase in the area exposed. The numbers near the bars represent the percentage changes
 640 relative to the baseline (only if greater than 1%).



641 **Table 1.** Total population exposed per sub-regions (million people/year).

Name	baseline	1.5 K	2 K	3 K
MEDITERRANEAN	14.4	16.8	18.8	21.7
ATLANTIC	16.0	16.1	19.5	24.5
CONTINENTAL	19.6	16.2	15.0	15.5
BOREAL	2.5	2.0	1.7	1.9
TOT	52.5	51.1	55.0	63.6

642

643 **Table 2.** Total agricultural land exposed per sub-regions (million ha/year).

Name	baseline	1.5 K	2 K	3 K
MEDITERRANEAN	5.8	7.1	8.0	9.6
ATLANTIC	5.4	5.5	6.3	7.6
CONTINENTAL	7.7	6.8	6.5	6.8
BOREAL	1.6	1.3	0.9	1.0
TOT	20.5	20.6	21.7	25.0

644